Mitochondria-dependent phase separation of disease-relevant proteins drives pathological features of age-related macular degeneration

Authors:

Nilsa La Cunza[1, 2, #], Li Xuan Tan[1, #], Thushara Thamban[1], Colin J. Germer[1,2], Gurugirijha Rathnasamy[3], Kimberly A. Toops[4] and Aparna Lakkaraju[1, 2, 5, *]

 # Equal Contribution.

Supplementary Information:

Supplementary Figures S1-S5

Legends for Supplementary Movies S1 - S8

Supplementary Table S1 – Reagents and sources

Supplementary Table S2 – Human donor demographics and AMD risk genotypes

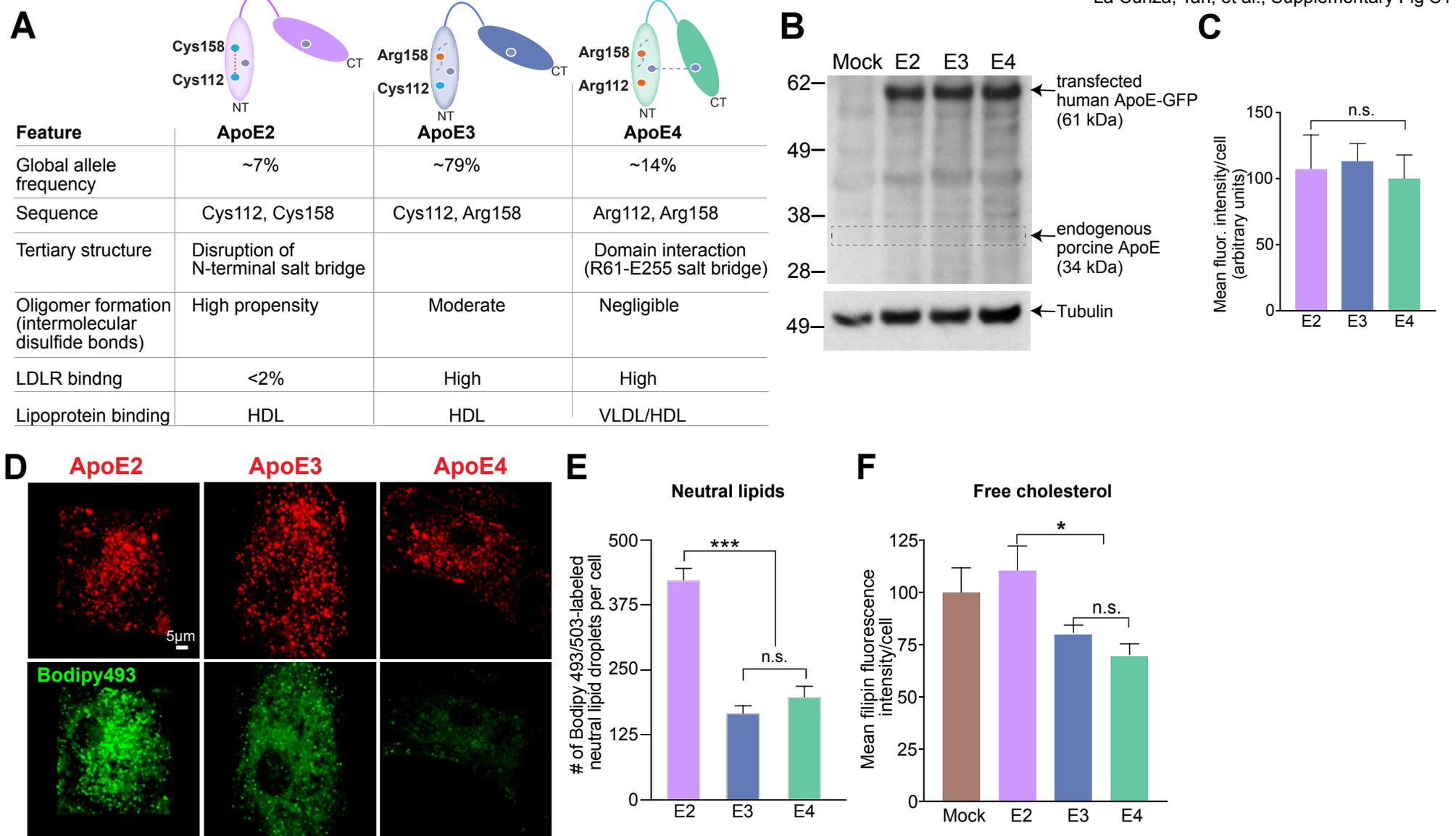**Supplementary Table S3 – Genotyping information**

Experimental Methods

References

A

| Feature	ApoE2	ApoE3	ApoE4
Global allele frequency	~7%	~79%	~14%
Sequence	Cys112, Cys158	Cys112, Arg158	Arg112, Arg158
Tertiary structure	Disruption of N-terminal salt bridge		Domain interaction (R61-E255 salt bridge)
Oligomer formation (intermolecular disulfide bonds)	High propensity	Moderate	Negligible
LDLR bindng	<2%	High	High
Lipoprotein binding	HDL	HDL	VLDL/HDL

Figure S1. Human ApoE isoforms - characteristics, expression, and lipid transport. (A) Structural features and of characteristics of human ApoE isoforms. Key amino acids at positions112 and 158 and potential intermolecular disulfide bonds (red dashed line) and salt bridges (gray dashed lines) are indicated. **(B)** Representative immunoblot of ApoE in porcine primary RPE transfected with EGFP-tagged human ApoE2, E3, or E4. Arrows: 61 kDa fusion proteins, 34 kDa endogenous ApoE and tubulin as loading control. **(C)** Quantification of mean mCherry fluorescence intensity per cell in primary RPE cultures transfected with mCherry-tagged ApoE2, E3 or E4. **(D)** Representative images from live imaging and **(E)** quantification of Bodipy 493/503-labeled neutral lipids in ApoE2, E3 or E4-expressing RPE. Mean ± SEM, n > 36 cells per condition, ***, $p < 0.0001$. **(F)** Primary RPE cultures were stained with filipin to label cholesterol and fluorescence intensity was quantified in cells expressing mCherry--tagged ApoE2, E3 or E4. Mean ± S.E.M. 17-23 cells per condition. One-way ANOVA with Bonferroni post-test*, $p < 0.05$, n.s., not significant.
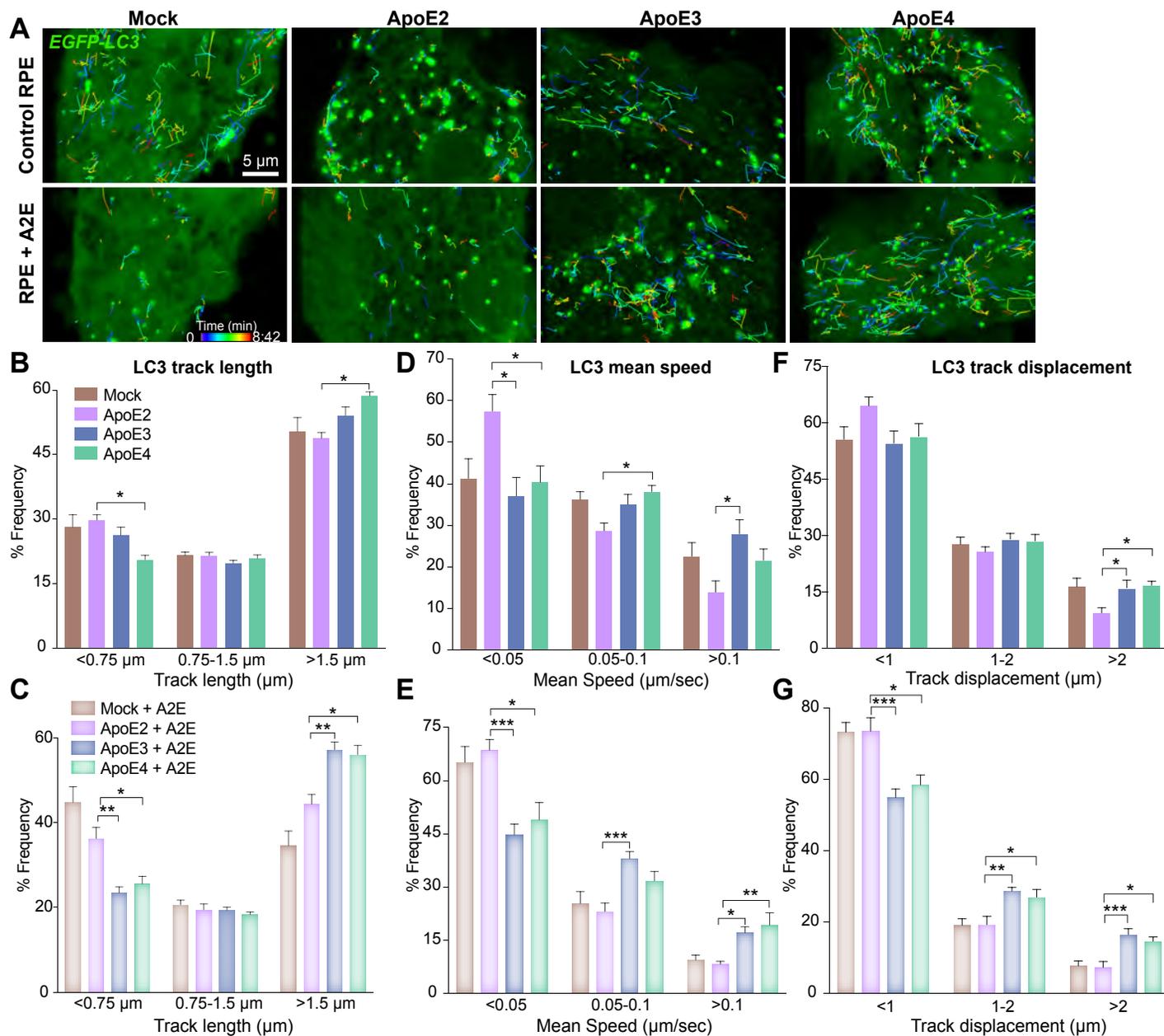
Supplementary Figure S2. ApoE4 restores autophagosome trafficking in RPE with lipofuscin. (A) Stills from live imaging of EGFP-LC3 autophagosomes (with spots and tracks superimposed) in mock-transfected or ApoE2, E3 or E4-expressing RPE, and treated or not with A2E. Frequency plots of EGFP-LC3 track lengths **(B)** & **(C)**, mean speeds **(D)** & **(E)**, and track displacements **(F)** & **(G)**. Mean ± SEM, n >13 cells/condition. One-way ANOVA with Bonferroni post-test. *, $p < 0.05$, **, $p < 0.005$, ***, and $p < 0.001$. See also Figure 2 and Movies S1-S8.
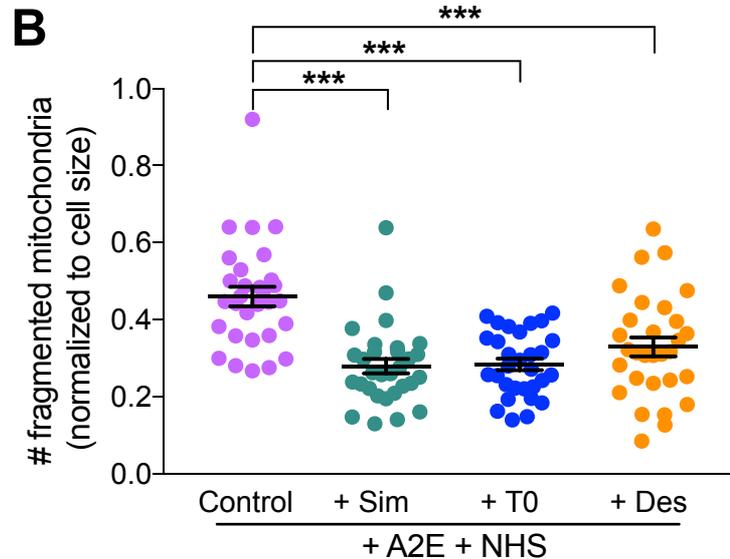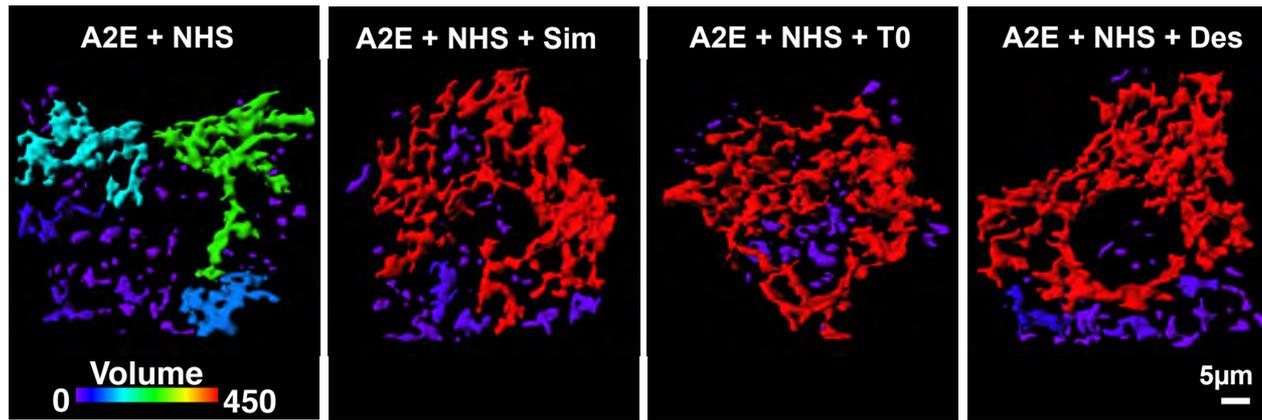
Figure S3. Drugs that lower cholesterol and ceramide prevent complement-induced mitochondrial fragmentation in RPE with A2E. (A) 3D reconstruction from live imaging of mitochondrial volumes in mock transfected RPE transduced with Mitotracker, treated with A2E and exposed to 10% NHS to induce complement attack. RPE were treated with Simvastatin (5 µM, 16 h), T0901317 (1 µM, 16 h) or desipramine (10 µM, 3 h) prior to imaging. Color bar: cooler colors indicate increasing mitochondrial fragmentation). **(B)** Number of fragmented mitochondria in (A). ***, $p < 0.0005$. Mean ± SEM, n = 30 cells per condition; One-way ANOVA with Bonferroni post-test; See also Figure 3.
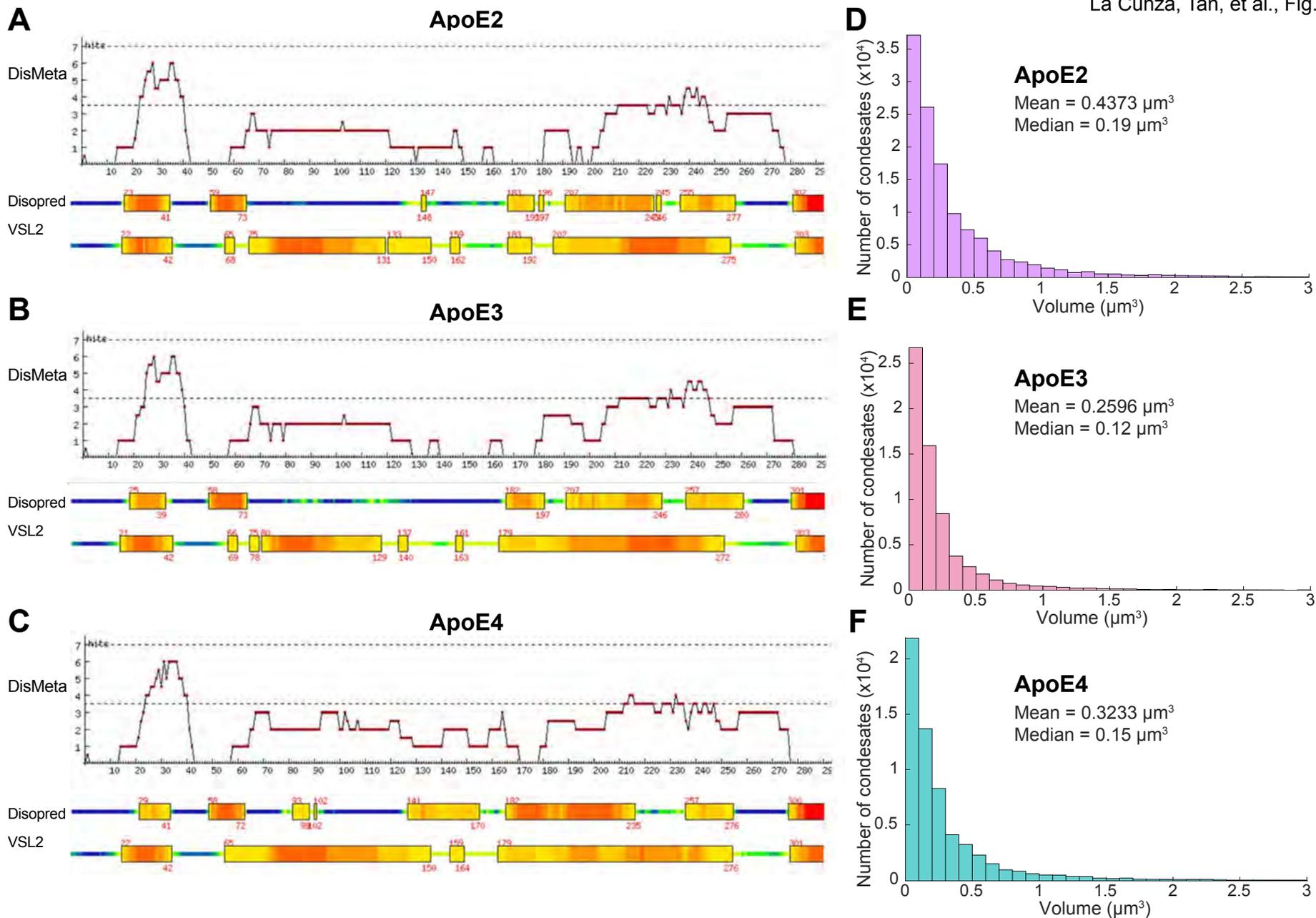
Figure S4. Phase separaton of ApoE isoforms. Index of disorder of **(A)** ApoE2, **(B)** ApoE3, and **(C)** ApoE4 predicted by a meta predictor of protein disorder (DisMeta), Disopred and VSL2 (Alberti et al., 2019). **(D), (E), and (F)** Histograms showing number and volumes of ApoE2, E3 or E4 condensates in primary RPE. Note the different scales for the Y-axes.
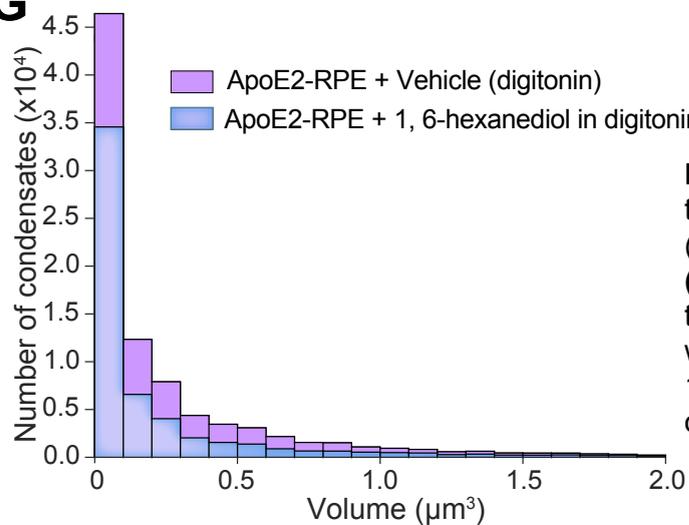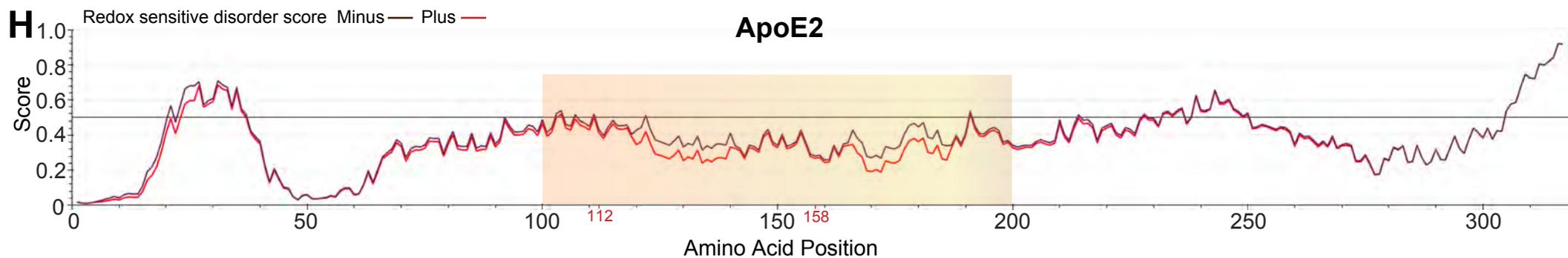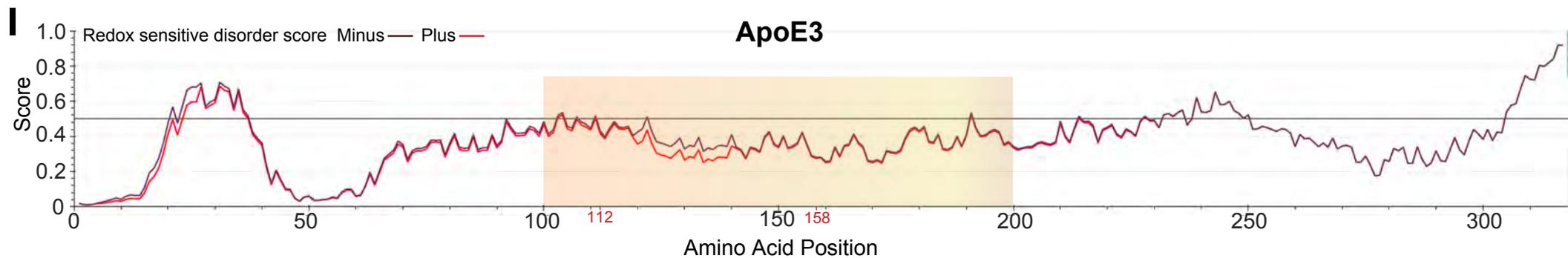
Figure S4. Phase separation of ApoE isoforms. (G) Number and volume of ApoE2 condensates in cells treated with 1,6-hexanediol, which disrupts weak hydrophobic interactions (blue bars) or with vehicle (digitonin, magenta bars) alone.

(H), (I) and (J) IUPRED disorder plots for ApoE2, E3 and E4 showing redox-state dependent order-disorder transitions (shaded areas). Note increased disorder in the region of 100-200 amino acids in ApoE2 **(H)** which spans the two cysteine residues at positions 112 and 158 (indicated in maroon), and between 100-150 in ApoE3 **(I)** that spans the cysteine at position 112. Also note lack of noticeable redox-sensitive order-disorder transition in ApoE4 **(J)**.
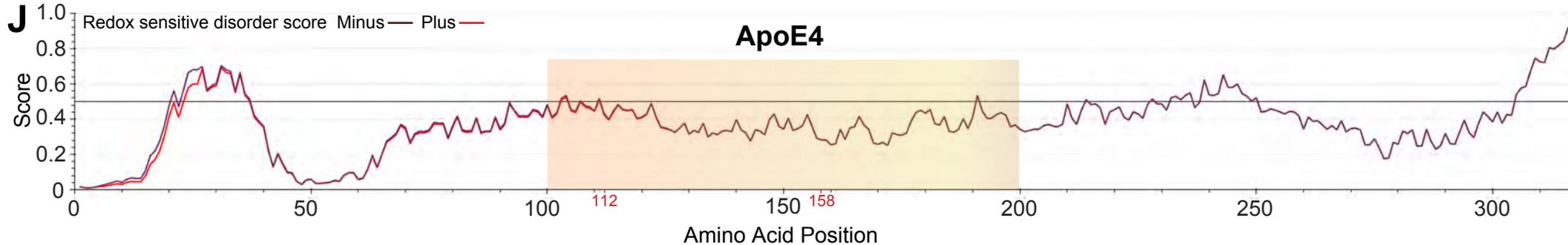
No primary control - TOM20
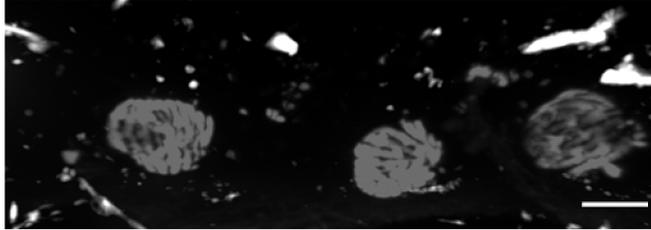
No primary control - ApoE
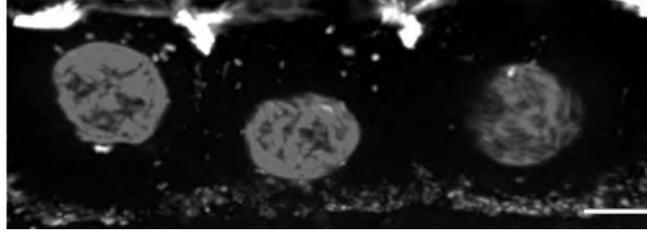
No primary control - p62

Figure S5. Antibody controls for immunostaining of human donor cryosections.
Representative images of immunostaining human donor cryosections incubated with secondary antibodies only. These images were used to control for any fluorescence due to endogenous tissue background (e.g., lipofuscin) and for non-specific binding of the secondary antibody to cellular components. Scale bar = 5 μm

Legends for Supplementary Movies

Movie S1: Live imaging of GFP-LC3 autophagosome trafficking in primary porcine RPE cultures by spinning disk microscopy.

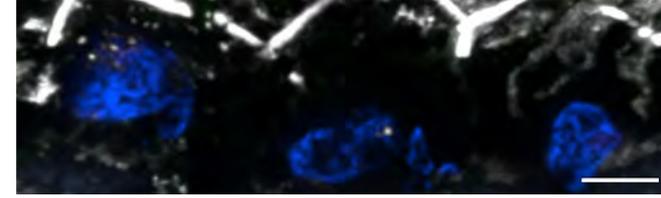**Movie S2:** Live imaging of GFP-LC3 autophagosome trafficking in A2E-treated primary porcine RPE cultures by spinning disk microscopy.

Movie S3. Live imaging of GFP-LC3 autophagosome trafficking in primary porcine RPE cultures expressing mCherry-ApoE2 by spinning disk microscopy.

Movie S4. Live imaging of GFP-LC3 autophagosome trafficking in A2E-treated primary porcine RPE cultures expressing mCherry-ApoE2 by spinning disk microscopy.

Movie S5. Live imaging of GFP-LC3 autophagosome trafficking in primary porcine RPE cultures expressing mCherry-ApoE3 by spinning disk microscopy.

Movie S6. Live imaging of GFP-LC3 autophagosome trafficking in A2E-treated primary porcine RPE cultures expressing mCherry-ApoE3 by spinning disk microscopy.

Movie S7. Live imaging of GFP-LC3 autophagosome trafficking in primary porcine RPE cultures expressing mCherry-ApoE4 by spinning disk microscopy.

Movie S8. Live imaging of GFP-LC3 autophagosome trafficking in A2E-treated primary porcine RPE cultures expressing mCherry-ApoE4 by spinning disk microscopy.

Table S1. Reagents and sources

REAGENT or RESOURCE			SOURCE	IDENTIFIER
Antibodies	**Host**	**IF or IB conc.**		
Acetylated Tubulin	Mouse	1:1,000	Sigma-Aldrich, St. Louis, MO	T6793
ApoE	Rabbit	1:200	GeneTex Inc, Irvine, CA	GTX100053
ApoE	Rabbit	1:300 (IB)	Dako, Glostrup, Denmark	A0077
Beta-tubulin	Mouse	1:1000	Sigma, St. Louis, MO	T5201
p62	Rabbit	1:200	Novus Biologicals, Littleton, CO	NBP148320
TOM20	Rabbit	1:200	Santa Cruz Biotechnology, Inc, Dallas, Texas	sc-11415
ZO-1	Rat	1:3000	(Xu et al., 2012 (1))	
Alexa Fluor Secondary antibodies (1:500) – various			ThermoFisher Scientific, Waltham, MA	

Plasmids		
pcDNA3.1 plasmids with human ApoE2, ApoE3 or ApoE4	Dr. Joachim Herz, UT Southwestern (2)
mCherry-ApoE2, E3 or E4	Generated in house from the pcDNA3.1 constructs and sequenced.
Biological Samples	
Human Eyes	Lions Gift of Sight, St Paul, MN
Biological samples: Cells	
Primary porcine RPE	Extracted from freshly harvested pig eyes obtained from Hart & Vold Meat Market, Baraboo, WI and Marin Sun Farms Inc., Petaluma, CA (3)

Biochemicals	**Source**	**Identifier**
Bovine Serum Albumin	Rockland Immunochemicals, Pottstown, PA	BSA-50
Calcium Chloride Dihydrate	Sigma-Aldrich, St. Louis, MO	C7902
DAPI (14.3 mM stock solution, used at 1:200)	Sigma-Aldrich, St. Louis, MO	D9542
Digitonin	Sigma Aldrich, St. Louis, MO	D141
dNTP mix	ThermoFisher, Waltham, MA	R72501

Glucose	Sigma Aldrich, St. Louis, MO	G7528
Glycerol	Sigma Aldrich, St. Louis, MO	G2025
GoTaq G2	Promega, Madison, WI	M7422
HBSS	Corning, Corning, NY	21-023-CV
HEPES	ThermoFisher, Waltham, MA	15630080
Magnesium Chloride Hexahydrate	Sigma-Aldrich, St. Louis, MO	M2393
NaCl	Sigma-Aldrich, St. Louis, MO	S5886
Paraformaldehyde (8%)	Electron Microscopy Sciences, Hatfield, PA	157-8
Phosphate Buffer Saline	ThermoFisher Scientific, Waltham, MA	BP665-1
Protease Inhibitors (used at 1:200)	Calbiochem, San Diego, CA	539134
Saponin	Sigma-Aldrich, St. Louis, MO	84510
Sucrose	Sigma-Aldrich, St. Louis, MO	S0389
Triton X-100	Sigma-Aldrich, St. Louis, MO	T8532
Trizma Base	Sigma-Aldrich, St. Louis, MO	RDD008
TrueBlack	Biotium, Fremont, CA	23007
Tween-20	Sigma-Aldrich, St. Louis, MO	P9416
VectaShield	Vector Laboratories, Burlingame, CA	H1000

Biochemicals: Components for porcine RPE cell culture		
Ciprofloxacin	Sigma-Aldrich, St. Louis, MO	17850-5G-F
DMEM	Corning, Corning, NY	10-013-CV
Fetal Bovine Serum (heat-inactivated)	American Type Culture Collection, Manassas, VA	30-2020
Non-essential amino acids (NEAA)	Corning, Corning, NY	25-025-CI
Penicillin-Streptomycin	Corning, Corning, NY	30-002-CI
0.25% Trypsin	Corning, Corning, NY	25-053-CI
2.5% Trypsin	Lonza, Walkersville, MD	17-160E

Biochemicals: Dyes

Bodipy 493/503	ThermoFisher, Waltham, MA	D3922
Filipin III	Sigma-Aldrich, St. Louis, MO	F4767
Mitotracker Far Red	ThermoFisher, Waltham, MA	M22426
Rhodamine phalloidin	Cytoskeleton Inc., Denver, CO	PHDR1

Biochemicals: Pharmacological treatments		
A2E	Synthesized and purified according to published protocols (4-6).	
Simvastatin	Cayman Chemicals, Ann Arbor, MI, USA	10010344
T0901317	Cayman Chemicals, Ann Arbor, MI, USA	71810
Desipramine Hydrochloride	Enzo Life Sciences, Farmingdale, NY	BML-AR119-0100
1,6 Hexanediol	Sigma Aldrich, St. Louis, MO	240117
Normal Human Serum	Quidel Corporation, San Diego, CA	A113

Critical Commercial Assays		
Amplex Red Cholesterol Assay Kit	ThermoFisher, Waltham, MA	A12216
DC protein assay kit	Bio-Rad Laboratories, Hercules, CA	5000112
PureLink® Genomic DNA Kit	ThermoFisher, Waltham, MA	K182001
Phusion™ High-Fidelity DNA Polymerase	ThermoFisher, Waltham, MA	F530S

Materials		
4-12% NuPAGE® Bis-Tris gels	Invitrogen, Carlsbad, CA	NP0321BOX
Embedding molds	ThermoFisher, Waltham, MA	50-465-348
T25 culture flasks	Corning, Corning, NY	353108
MatTek dish (35mm)	MatTek Corporation, Ashland, MA	P35G-1.5-14-G
TissueTek OCT	Radnor Corporate Center, Radnor, PA	25608-930

Transduction reagents		

Premo Autophagy LC3B-GFP	ThermoFisher, Waltham, MA	P36235

Software and Algorithms		
GraphPad Prism 8	GraphPad Prism®, La Jolla, CA	
Image Studio Lite Ver. 5.2.5	LI-COR, Lincoln, NE	
Imaris v 8.7.4	Bitplane, Concord, MA	
Matlab R2020a	MathWorks, Natick, MA	

Table S2. Demographic and genotyping information of human donors
(Risk allele is in red)

Donor #	Donor Id#	Donor demographics	Clinical diagnosis	APOE	CFH	C3	HTRA1	ARMS2	Cause of death	Death to preservation
1	996	65 (Male, Caucasian)	Control	E3/E4 rs429358 C/T rs7412 C/C	**C**T	C**G**	GG	GG	Lung cancer	10 hours
2	226	76 (Male, Caucasian)	Control	E3/E3 rs429358 T/T rs7412 C/C	TT	C**G**	**A**G	G**T**	Respiratory failure, pneumonia	13 hours
3	684	94 (Female, Caucasian)	Control	E3/E3 rs429358 T/T rs7412 C/C	TT	CG	GG	GG	Colon cancer	7 hours
4	236	95 (Female, Caucasian)	AMD	E3/E3 rs429358 T/T rs7412 C/C	**C**T	C**G**	GG	GG	Small bowel obstruction	6 hours
5	1004	84 (Male, Caucasian)	AMD	E3/E3 rs429358 T/T rs7412 C/C	**C**T	CC	GG	G**T**	Respiratory failure	6 hours
6	1061	82 (Male, Caucasian)	AMD	E3/E4 rs429358 C/T rs7412 C/C	TT	C**G**	**A**G	G**T**	Abdominal aortic aneurysm	6 hours

Table S3. PCR primers and conditions for genotyping

Gene	SNP	Primer	PCR Conditions	Size (bp)
CFH Y402H	rs1061170	F: 5'- TCATTGTTATGGTCCTTAGGAAA-3' R: 5'- TTAGAAAGACATGAACATGCTAGG-3'	98ºC for 3 min, 98ºC for 10 sec, 58ºC for 45 sec, 72ºC for 45 sec, 72ºC for 7 min; 34 cycles	241
C3 R102G	rs2230199	F: 5'- GACAAAGAGGCCTCGTGAGA-3' R: 5'- GACCAAGAATAATGGGCAGGC-3'	98ºC for 3 min, 98ºC for 10 sec, 64ºC for 20 sec, 72ºC for 20 sec, 72ºC for 5 min; 34 cycles	348
ARMS2	rs10490924	F: 5'- TACCCAGGACCGATGGTAAC-3' R: 5'-GAGGAAGGCTGAATTGCCTA-3	98ºC for 3 min, 98ºC for 10 sec, 58ºC for 20 sec, 72ºC for 40 sec, 72ºC for 7 min; 35 cycles	449
HTRA1	rs11200638	F: 5'- CTAGGCTCTCTGCGAATACGG-3' R: 5'- ATGGAACTTTGCAAGGGGGC-3'	98ºC for 3 min, 98ºC for 10 sec, 64ºC for 20 sec, 72ºC for 20 sec, 72ºC for 5 min; 34 cycles	396
APOE	rs429358 & rs7412	F: 5'-TCGGAACTGGAGGAACAACT-3' R: 5'-ACCTGCTCCTTCACCTCGT-3'	98ºC for 3 min, 98ºC for 10 sec, 64ºC for 20 sec, 72ºC for 20 sec, 72ºC for 5 min; 34 cycles	482

Experimental Methods

Primary porcine RPE cell cultures

RPE were isolated from porcine retinas using established protocols (3). Briefly, the anterior segment was removed at the *ora serrata*, and the retina was gently detached by clipping at the optic nerve head. RPE cells were isolated from eyecups upon incubation with 0.5% trypsin (Lonza, Walkersville, MD) with 5.3 mM EDTA in Hank's balanced salt solution (Corning, Corning, NY) and plated onto T25 flasks in growth medium (DMEM with 4.5 g/L glucose, 1% heat-inactivated fetal bovine serum, 1% non-essential amino acids and 1% penicillin/streptomycin). For live imaging, RPE were plated at confluence (~ 300,000 cells/cm^2) on serum-coated glass-bottom dishes (Mattek) as described (3, 5).

Treatments and assays

Pharmacological treatments were performed as previously described (3, 7, 8). Cells were treated with 10 µM bisretinoid A2E for 6 h followed by a 48-h chase in fresh culture medium. The LXR agonist T0901317 (Cayman Chemicals, Ann Arbor, MI) was used at 1 µM for 16 h, the ASMase inhibitor desipramine hydrochloride was used at 10 µM for 3 h and the lipophilic statin simvastatin (Cayman Chemicals, Ann Arbor, MI) was used at 5 µM for 16 h. Total cell cholesterol levels were measured with the Amplex Red cholesterol assay (ThermoFisher) as detailed previously (5, 6).

ApoE constructs

pcDNA3.1 plasmids expressing human ApoE2, E3 and E4 were provided by Dr. Joachim Herz (University of Texas Southwestern Medical Center, Dallas, TX) (2). The mCherry-tagged constructs were generated by inserting the ApoE2, E3 or E4 cDNA into the p-mCherry-N1 vector (Invitrogen) between the XhoI and BamHI restriction sites. Sequences of the constructs was confirmed by UW-Madison Biotechnology Core and by Quintara (South San Francisco, CA).

Transfections

Primary porcine RPE were transfected with mCherry-tagged ApoE2, E3 or E4 using the Amaxa nucleofector II (Lonza, Rockland, ME). Approximately 1.5 million cells and 5 µg plasmid DNA were used for each transfection. Cells were plated at confluence (300,000 cells/sq.cm) in growth

medium on serum-coated glass-bottom dishes (MatTek, Ashland, MA) and used for live imaging 48-72 h later. Transfection efficiencies were ~30-40% for each of the isoforms.

Live imaging and analysis of ApoE trafficking

mCherry-ApoE2, E3 or E4 expressing primary porcine RPE cell cultures were imaged in recording medium (1 x HBSS, 4.5 g/L glucose, 0.01 M HEPES) supplemented with 1% FBS and 1% NEAA as described previously (2,4,5). Rapid Z-stacks were acquired using the Andor Revolution XD with 100x/1.49 NA Apo TIRF objective (Nikon, Melville, NY) for ~50 frames at 37°C. Trafficking data were collected from three separate transfections for a total of at least 17–23 movies captured per condition. During image acquisition, care was taken to maintain the same laser power, exposure and electron-multiplying gain settings. Images were subjected to background subtraction and Gaussian smoothing (same settings for all images within a set of experiments) in Imaris v 8.7.4 (Bitplane, Concord, MA). For analysis of trafficking parameters, ApoE-labeled vesicles were subjected to surface reconstruction using the Surfaces and Tracks modules, with the same intensity threshold applied to all images within a set of experiments. Track length, track displacement and track lifetimes were exported and statistical analysis of these data sets was performed using Prism (GraphPad, La Jolla, CA).

Immunoblotting

For ApoE immunoblotting, primary porcine RPE pellets were lysed in 1X HNTG lysis buffer (50mM HEPES, 150mM NaCl, 10% glycerol, 1.5mM MgCl2, 1% Triton X-100) supplemented with protease inhibitors (1:200, Calbiochem, San Diego, CA, 539134) by sonication for 10 min. Protein measurements were performed using DC assay kit (Bio-Rad Laboratories, Hercules, CA). 30 μg of lysates per condition were resolved in 4-12% NuPAGE® Bis-Tris Precast gels (Invitrogen, Carlsbad, CA) at 130 V for ~1.5 h, transferred onto nitrocellulose membrane with iBlot dry transfer system (Thermo Fisher, Waltham, MA). Membranes were blocked with 5% milk in Tris buffered saline with Tween20 (TBS-T) for 1 h before being incubated in primary antibody overnight at 4ºC. Membrane was probed with antibodies to rabbit anti-human ApoE (1:300; Dako, #A0077, Glostrup, Denmark), mouse-anti beta-tubulin (1:1000; Sigma #T5201, St. Louis, MO) followed by washes in TBS-T and incubated with horseradish peroxidase-conjugated secondary antibodies (1:5000) for 1 h. After immunoblots were visualized by ECL substrate (Thermo

Fisher, Waltham, MA), bands were quantified using Image Studio (LI-COR, Lincoln, NE) and ApoE levels were normalized to that of beta-tubulin.

Neutral lipid staining with Bodipy 493/503

mCherry-ApoE2, E3 or E4 expressing primary porcine RPE cell cultures were treated with Bodipy-493/503 (10 µM for 30 min at 37ºC). Cells were washed, fixed in 2% paraformaldehyde and imaged using the Andor Revolution XD with 100x/1.49 NA Apo TIRF objective (Nikon, Melville, NY). The number of Bodipy493/503 positive vesicles were quantified by the Spots module (Imaris). Statistical analysis of these data sets was performed using Prism (GraphPad, La Jolla, CA).

Free cholesterol staining with filipin

mCherry-ApoE2, E3 or E4 expressing primary porcine RPE cell cultures were fixed with 2% paraformaldehyde and stained with 50 µg/ml filipin for 45 min (F4767, Sigma-Aldrich, St. Louis, MO) and imaged using the Andor Revolution XD with 100x/1.49 NA Apo TIRF objective (Nikon, Melville, NY). Intracellular filipin fluorescence was quantified by using Imaris. Statistical analysis of these data sets was performed using Prism (GraphPad, La Jolla, CA).

Live imaging of autophagosome biogenesis and trafficking

mCherry-ApoE2, E3 or E4 expressing primary porcine RPE cell cultures were transduced at 6.7 transducing units/cell of Premo Autophagy LC3B-GFP (ThermoFisher, Waltham, MA) for 16-24 hours. Cells were serum starved 2 h to induce autophagy and imaged in recording medium (1 x HBSS, 4.5 g/L glucose, 0.01 M HEPES) supplemented with 1% FBS and 1% NEAA as described previously (5). Time-lapse movies were acquired using the Andor Revolution XD with 100x/1.49 NA Apo TIRF objective (Nikon, Melville, NY) for ∼50 frames (50 millisecond exposure) at 37°C. Trafficking data were collected from three separate transfections for a total of at least 12–15 movies captured for treatment. Identical laser power, exposure and gain settings were applied within the same set of experiments. Images were subjected to background subtraction and Gaussian smoothing (same settings for all images within a set of experiments) in Imaris v 8.7.4 (Bitplane, Concord, MA). For analysis of organelle numbers and trafficking parameters, LC3B-labeled autophagosomes were subjected to spots reconstruction using the Spots and Tracks

modules, with the same intensity threshold applied to all images within a set of experiments. Numbers, track length, track mean speed and track displacement length were exported and statistical analysis of these data sets was performed using Prism (GraphPad, La Jolla, CA) as described previously (5).

Acetylated tubulin staining and quantification

mCherry-ApoE2, E3 or E4 expressing primary porcine RPE cell cultures were treated or not with A2E (10 μM for 6 h followed by a 48-h chase in fresh culture medium). Cells were fixed in 2% paraformaldehyde for 10 min at RT, rinsed in PBS with Ca^{2+} and Mg^{2+} (1x PBS with 1M $MgCl_2$ and 1M $CaCl_2$; PBS C/M), blocked in 1% bovine serum albumin (BSA) in PBS C/M, and incubated with specific primary antibodies diluted in 1% BSA in PBS C/M and 1% saponin for 1 h: mouse monoclonal anti-acetylated tubulin clone 6-11B-1 (1:1000; Sigma-Aldrich), and rat anti-ZO1 (1:3000; Xu et al., 2012). Alexa Fluor secondary antibodies were used at 1:500 and DAPI (1:200; Sigma-Aldrich, St. Louis, MO). Cells were imaged with an Andor Revolution XD with 100x/1.49 NA Apo TIRF objective (Nikon, Melville, NY) with identical exposures and gains for each antibody. For each transfected cell, a region of interest (ROI) was drawn just within the plasma membrane, and the acetylated tubulin fluorescence intensity per pixel of the ROI per plane of the confocal image stack was quantified by Imaris. Statistical analysis of these data sets was performed using Prism (GraphPad, La Jolla, CA).

Live imaging of mitochondrial dynamics

mCherry-ApoE2, E3 or E4 expressing primary porcine RPE cell cultures $\pm$ A2E (10 μM for 6 h followed by a 48-h chase in fresh culture medium) were exposed to 10% NHS for 10 min (on day 1 and day 3, with a rest on day 2 (8)). Cells then incubated with 0.2 μM MitoTracker Deep Red (ThermoFisher, Waltham, MA) for 15 min at 37ºC and imaged immediately. Some cultures were treated with the LXR agonist T0901317 (Cayman Chemicals, Ann Arbor, MI) at 1 μM for 16 h or the ASMase inhibitor desipramine hydrochloride at 10 μM for 3 h or the lipophilic statin simvastatin (Cayman Chemicals, Ann Arbor, MI) at 5 μM for 16 h. RPE cells were incubated with 0.2 μM MitoTracker Deep Red (ThermoFisher, Waltham, MA) for 15 min at 37ºC immediately prior to imaging. Cells were imaged in recording medium (1 x HBSS, 4.5 g/L glucose, 0.01 M HEPES) supplemented with 1% FBS and 1% NEAA as described previously (8) on the Andor

Revolution XD with 100x/1.49 NA Apo TIRF objective (Nikon, Melville, NY) with 50 millisecond exposure at 37°C. Identical laser power, exposure and gain settings were applied within the same set of experiments. Images were subjected to background subtraction and Gaussian smoothing (same settings for all images within a set of experiments) in Imaris v 8.7.4 (Bitplane, Concord, MA). For analysis of mitochondrial volume, MitoTracker-labeled mitochondria were subjected to surface reconstruction using the Surfaces and Tracks modules, with the same intensity threshold applied to all images within a set of experiments. The Surface module takes a 3D data set, as from confocal imaging, and uses an object identification algorithm with user defined threshold criteria to build artificial solid objects within the image that can be measured for statistics such as the number of discrete or connected objects and the object's volumes. Automated segmentation of these objects by color-coding, based on volume of the connected components, was used for 3D surface rendering of these objects. Statistical analysis of these data sets was performed using Prism (GraphPad, La Jolla, CA).

Analysis of ApoE condensate volumes

For analysis of ApoE condensate volumes, mCherry-ApoE2, E3 or E4 expressing primary porcine RPE cell cultures were imaged live using the same imaging conditions and parameters established for imaging ApoE trafficking. The mCherry-ApoE structures were subjected to surface reconstruction using the Surfaces and Tracks modules, with the same intensity threshold applied to all images within a set of experiments. For each transfected cell, a region of interest (ROI) was drawn and the mCherry fluorescence intensity per pixel of the ROI per plane of the confocal image stack was quantified by Imaris. Volumes were exported from the Statistics tab. Histograms of number and volumes of ApoE condensates were created by Matlab (MathWorks, Natick, MA). Statistical analysis of these data sets was performed using Prism (GraphPad, La Jolla, CA).

Analysis of ApoE condensates after 1,6-hexanediol treatment

mCherry-ApoE2 expressing primary porcine RPE cell cultures were treated with 5 μg/mL digitonin alone (control) for 15 min or 5 μg/mL digitonin (Sigma Aldrich, St. Louis, MO) for 13 min with the aliphatic alcohol, 0.5% 1,6 hexanediol (Sigma Aldrich, St. Louis, MO) added for the last 2 min of the 15 min treatment (9). Cells were imaged in recording medium (1 x HBSS, 4.5 g/L glucose, 0.01 M HEPES) supplemented with 1% FBS and 1% NEAA using spinning disk confocal

microscopy (Nikon CSU-X1 dual camera platform equipped with Okolab stagetop incubation system: specifically, the iXon Ultra 888 EM-CCD camera) using a 100X Apo TIRF 1.49 NA oil objective for ~25 frames (50 millisecond exposure) at 37ºC. Identical laser power, exposure and gain settings were applied within the same set of experiments. Images were subjected to background subtraction and Gaussian smoothing (same settings for all images within a set of experiments) in Imaris v 8.7.4 (Bitplane, Concord, MA). For analysis of numbers and volume, ApoE condensates were subjected to surface reconstruction using the Surfaces and Tracks modules, with the same intensity threshold applied to all images within a set of experiments. Histogram of number and volumes of ApoE2 condensates was created by Matlab (MathWorks, Natick, MA). Statistical analysis of these data sets was performed using Prism (GraphPad, La Jolla, CA).

Live imaging of ApoE condensate fusion

mCherry-ApoE2, E3 or E4 expressing primary porcine RPE cell cultures were imaged on a spinning disk confocal microscope (Nikon CSU-X1 dual camera platform equipped with Okolab stagetop incubation system: specifically, the iXon Ultra 888 EM-CCD camera) using a 100X Apo TIRF 1.49 NA oil objective at 37ºC. To capture ApoE condensate fusion events, time-lapse movies were acquired at 9 s intervals for 24 seconds (50 millisecond exposure) at 37°C. Identical laser power, exposure and gain settings were applied within the same set of experiments. Images were subjected to background subtraction and Gaussian smoothing (same settings for all images within a set of experiments) in Imaris v 8.7.4 (Bitplane, Concord, MA).

Mice

Wild-type (Jackson Labs 129S1/SvImJ) and $Abca4^{-/-}$ mice (Jackson Labs Abca4tm1Ght/J) both on Rpe65 Leu450 background were raised under 12-h cyclic light with standard diet. Mice (~6-10 months, both sexes) were euthanized ~3 h after light onset. Eyes were enucleated, and eyecups were processed for immunofluorescence staining as detailed previously (5, 7, 8). For desipramine studies, mice were intraperitoneally injected thrice a week for four weeks with either 100 µl sterile, distilled water or 10 mg/kg of desipramine hydrochloride (Enzo Life Sciences, Farmingdale, NY) dissolved in sterile, distilled water (7). All studies were approved by the University of California-San Francisco animal care and use authorities.

Human donor eyes

Globes from unaffected human donors and donors diagnosed with AMD were obtained from Lions Gift of Sight (Saint Paul, MN) with de-identified demographics (Table S2) and fundus photographs. Globes were enucleated within 6-10 hours after death, fixed in 4% PFA and shipped in normal saline. The anterior portions of the globe were removed by cutting along the *ora serrata* and the cornea, lens and vitreous were discarded. The eyecups were infiltrated with 10%, 20%, 30% sucrose in phosphate buffer for 30 min each, followed by 4:1 30% sucrose:OCT and 2:1 30% sucrose:OCT for 30 min each. The macula and periphery regions of the RPE were separated, frozen in TissueTek OCT in embedding molds and sectioned into 20 µm cryosections using a Leica microtome.

Genotyping of human donor tissue

DNA samples from flash frozen human eye globes (Lions Gift of Sight) were extracted from ~20 mg eye tissue by using the PureLink Genomic DNA Kit (ThermoFisher, Waltham, MA) according to the manufacturer's instructions. DNA was diluted with nuclease free water to 40 ng/µL for genotyping analysis. PCR amplification was performed as follows for each SNP. For ABCA1 and CETP, reactions were carried out in a total volume of 20µL containing 40-50 ng DNA, 10pM of each primer, GoTaq G2 buffer, and nuclease free water. For CFH Y402H, reactions were carried out in a total volume of 20 µL containing 40 ng DNA, 2.5 mM dNTP mix, 10 µM of each primer, 5x Phusion GC Buffer, Phusion DNA polymerase (2 U/µL) and nuclease free water. For the other variants, reactions were carried out in a total volume of 20 µL containing 40 ng DNA, 2.5 mM dNTP mix, 10 µM of each primer, 5x Phusion GC Buffer, 100% DMSO, Phusion DNA polymerase (2 U/µL) and nuclease free water. Phusion™ High-Fidelity DNA Polymerase kit (ThermoFisher, Waltham, MA) was used according to the manufacturer's instructions. The PCR primers and conditions are summarized in Table S3 (10-12). All PCR products were sent to Quintara (South San Francisco, CA) for Sanger sequencing and the genotyping results are in Table S2.

Immunofluorescence staining of human and mouse cryosections

Cryosections were thawed for 10 min at room temperature. Cryosections were blocked in 4% BSA (Rockland Immunochemicals, Pottstown, PA) in PBS (ThermoFisher, Waltham, MA) for 2.5 hrs at room temperature. After three washes in 1% BSA in PBS, cryosections were incubated with the

following antibodies in 1% BSA in PBS at 4ºC for 48 h in a humidified chamber (rabbit anti-ApoE (Genetex; 1:200), rabbit anti-p62/SQSTM1 (Novus; 1:200) and rabbit anti-TOM20 (Santa Cruz; 1:200)). Sections were washed three times with PBS to remove unbound antibodies, and incubated with AlexaFluor secondary antibodies (1:500, ThermoFisher Scientific, Waltham, MA) (16 h, 4ºC for human and 2 h at room temperature for mouse cryosections). After one wash in PBS with 1% BSA, the sections were incubated with Rhodamine phalloidin (14 μM; 1:200, Cytoskeleton Inc, Denver, CO, PHDR1) (30 min, RT) and DAPI (14.3 mM; 1:200, Sigma-Aldrich, St. Louis, MO, D9542) (10 min, RT). Human cryosections were treated with TrueBlack reagent (Biotium, Fremont, CA, 23007) for 30 s after immunostaining and rinsed with PBS (3 times, 5 mins each) to quench lipofuscin autofluorescence. Cryosections were mounted under glass coverslips with PBS and Vectashield (Vector Laboratories, Burlingame, CA). Sections were imaged on a spinning disk confocal microscope (Nikon CSU-X1 dual camera platform using the Photometrics Prime 95B Back-illuminated sCMOS) using a 100X Apo TIRF 1.49 NA oil objective with identical exposures and gains for each antibody.

Analysis of mitochondrial volumes and protein condensates

Human donor cryosections and mouse RPE flatmounts were immunostained with antibodies to Tom20 (1:200, Santa Cruz), ApoE (Genetex; 1:200) or p62 (1:200, Novus) and analyzed with Imaris 9.6 (Bitplane). Images were subjected to Gaussian filtering and background subtraction. Surface reconstructions were made with the "Surfaces" module. Mean volumes and areas were exported from the statistics tab and analyzed in Excel and Prism.

Statistics

Data were analyzed by using either a one-way or two-way ANOVA with the Bonferroni post hoc test or a multiple t-test with Welch's correction for unequal variances (GraphPad Prism). Unless otherwise stated, data are presented as mean ± SEM of ≥3 independent experiments, with at least two to three replicates per condition per experiment.

References:

1. Xu J, Toops KA, Diaz F, Carvajal-Gonzalez JM, Gravotta D, Mazzoni F, et al. Mechanism of polarized lysosome exocytosis in epithelial cells. *J Cell Sci.* 2012;125(Pt 24):5937-43.
2. Chen Y, Durakoglugil MS, Xian X, and Herz J. ApoE4 reduces glutamate receptor function and synaptic plasticity by selectively impairing ApoE receptor recycling. *Proc Natl Acad Sci U S A.* 2010;107(26):12011-6.
3. Toops KA, Tan LX, and Lakkaraju A. A detailed three-step protocol for live imaging of intracellular traffic in polarized primary porcine RPE monolayers. *Exp Eye Res.* 2014;124C:74-85.
4. Parish CA, Hashimoto M, Nakanishi K, Dillon J, and Sparrow J. Isolation and one-step preparation of A2E and iso-A2E, fluorophores from human retinal pigment epithelium. *Proc Natl Acad Sci U S A.* 1998;95(25):14609-13.
5. Toops KA, Tan LX, Jiang Z, Radu R, and Lakkaraju A. Cholesterol-mediated activation of acid sphingomyelinase disrupts autophagy in the retinal pigment epithelium. *Mol Biol Cell.* 2015;26:1-14.
6. Lakkaraju A, Finnemann SC, and Rodriguez-Boulan E. The lipofuscin fluorophore A2E perturbs cholesterol metabolism in retinal pigment epithelial cells. *Proc Natl Acad Sci U S A.* 2007;104(26):11026-31.
7. Kaur G, Tan LX, Rathnasamy G, La Cunza NR, Germer CJ, Toops KA, et al. Aberrant early endosome biogenesis mediates complement activation in the retinal pigment epithelium in models of macular degeneration. *Proc Natl Acad Sci U S A.* 2018;115:9014-9.
8. Tan LX, Toops KA, and Lakkaraju A. Protective responses to sublytic complement in the retinal pigment epithelium. *Proc Natl Acad Sci U S A.* 2016;113(31):8789-94.
9. Gopal PP, Nirschl JJ, Klinman E, and Holzbaur EL. Amyotrophic lateral sclerosis-linked mutations increase the viscosity of liquid-like TDP-43 RNP granules in neurons. *Proc Natl Acad Sci U S A.* 2017;114(12):E2466-E75.
10. Ferrington DA, Kapphahn RJ, Leary MM, Atilano SR, Terluk MR, Karunadharma P, et al. Increased retinal mtDNA damage in the CFH variant associated with age-related macular degeneration. *Exp Eye Res.* 2016;145:269-77.
11. Fritsche LG, Igl W, Bailey JN, Grassmann F, Sengupta S, Bragg-Gresham JL, et al. A large genome-wide association study of age-related macular degeneration highlights contributions of rare and common variants. *Nat Genet.* 2016;48(2):134-43.
12. Abbas RO, and Azzazy HM. Association of single nucleotide polymorphisms in CFH, ARMS2 and HTRA1 genes with risk of age-related macular degeneration in Egyptian patients. *Ophthalmic Genet.* 2013;34(4):209-16.